CAA
2018

Clément Laplaige et al.
https://dx.doi.org/10.15496/publikation-87772

Extraction of Linear Structures from LIDAR Images Using a Machine Learning Approach

Clément Laplaige
UMR 7324 CITERES-LAT
Université de Tours,
clement.laplaige@univ-tours.fr

Jean-Yves Ramel
LIFAT, Université de Tours.
jean-yves.ramel@univ-tours.fr

Xavier Rodier
UMR 7324 CITERES-LAT
Université de Tours, CNRS
xavier.rodier@univ-tours.fr

Shuo Bai
LIFAT, Université de Tours
shuo.bai@etu.univ-tours.fr

Ronan Guillaume
LIFAT, Université de Tours
ronan.guillaume@etu.univ-tours.fr

Abstract

LiDAR (Light Detection And Ranging) technology makes it possible to generate highly accurate elevation models from the ground whatever the nature of the plant cover. LiDAR elevation models have proliferated during the past decade, delivering an unprecedented number of original archaeological finds in the forest. These include habitat, agricultural or funeral structures prior to the existence of forest cover, and also archaeological micro-structures directly linked to past forest economy.

Until recently, LiDAR acquisitions in France were limited to small areas. However, the recent and rapid supply of large-scale reference data by the National Geographic Institute provides large amounts of very high-resolution data about areas covering several thousand square kilometers that were previously little known from an archaeological point of view. Manual digitization of remains is a time-consuming activity and does not guarantee exhaustive recognition of features.

As part of the "SOLiDAR" project (a tribute to the federation of unions Solidarność) (http://citeres.univ-tours.fr/spip.php?article2133), we present a Machine Learning approach enabling reliable and flexible extraction and characterization of archaeological structures discovered in the LiDAR datasets. We have developed an open human-machine interface (HMI) that is accessible to the majority of archaeologists. This system, far from being a "black box", can automatically process the remains but can also be used step by step, leaving the user to decide whether or not to validate the different processing parameters.

Keywords: LiDAR, Automated detection, Machine learning

Introduction

LiDAR technology makes it possible to generate highly accurate elevation models from the ground whatever the nature of the plant cover. It is thus possible to detect many archaeological remains related, for example, to habitat, agricultural or funeral structures.

Over and above Digital Elevation Models (DEM) or Digital Terrain Models (DTM), ground surface data obtained by Lidar surveys provide useful information about how the landscape has evolved. They can be an indirect indicator of the consequences on populations today of human activities over the long term (from earliest times to the present day).

To extract and characterize archaeological structures from LiDAR data, most studies have focused on manual identification or automatic image processing (IP). More recently, there has been an increase in the number of studies conducted on semi-automated methods based on machine learning (ML). This paper describes first the archaeological issues under-

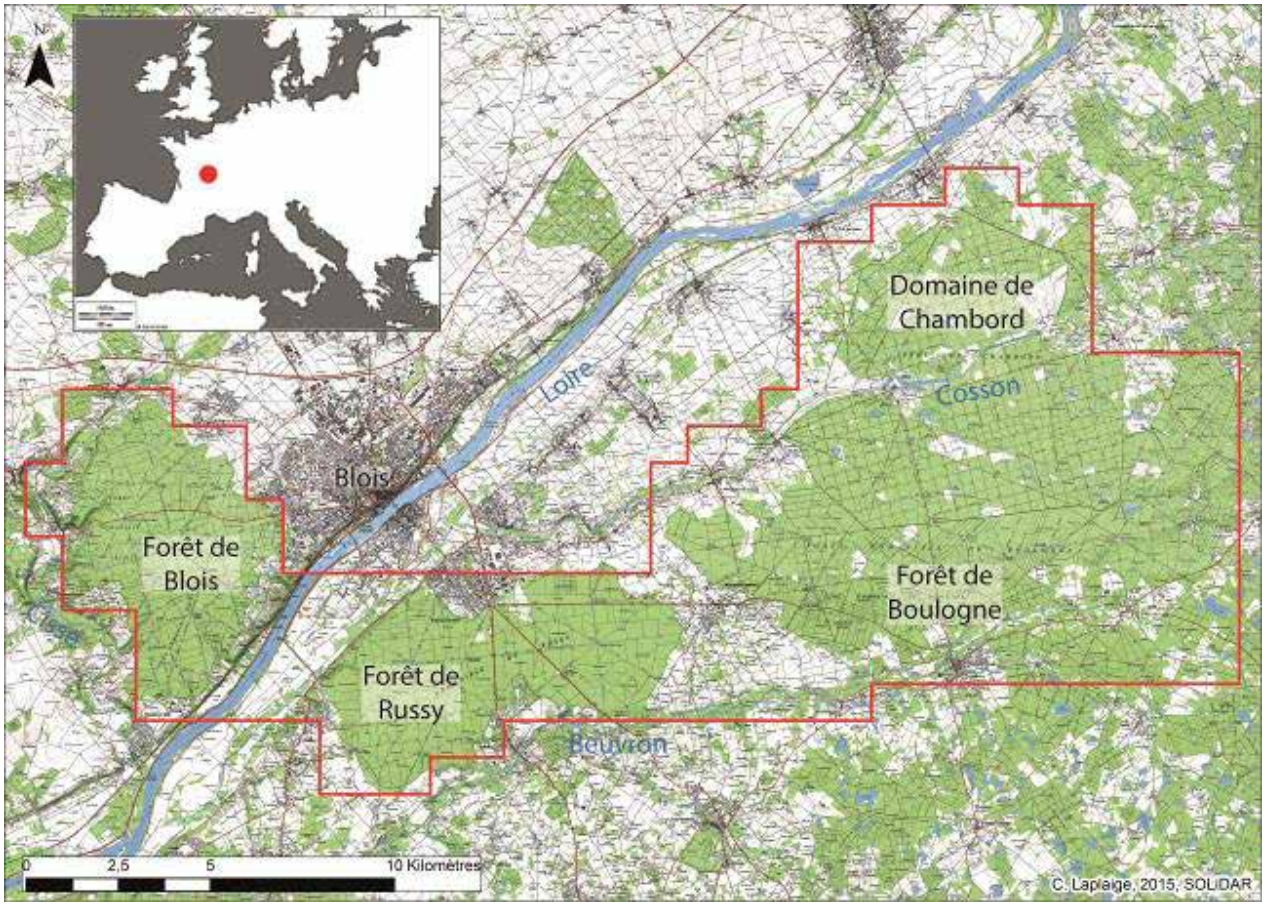

Figure 1. Location map of the study area.

lying the SOLiDAR project and the use of conventional image processing techniques. It then presents a machine learning approach aimed at obtaining better and more flexible extraction of archaeological structures from LiDAR derivatives. The article is organized as follows: (1) the background of the work and the software that we have developed, (2) the remains investigated, (3) the data processing, and (4) the first results.

Research Context, Study Area, Data Sources and Development of Software

There are many methods for automatically processing LiDAR data; the best known is pixel analysis (Sevara et al. 2016). In the last ten years, work by geographers and computer scientists has led to more efficient methods, such as template matching and segmentation (Baatz, Hoffmann and Willhauck 2008; Blaschke 2010; Martha et al. 2010; Sevara et al. 2016).

The use of Machine Learning (Chen et al. 2014; Duro, Franklin and Dubé 2012; Li et al. 2015) has received growing attention because of the increasing availability of easy-to-use libraries and software. For example, Martha et al. used optical images for segmentation and auxiliary elevation data for landslide detection (Martha et al. 2010); Anders et al. used LiDAR DEM-derived features for geomorphological change detection (Anders, Seijmonsbergen and Bouten 2013); Eisank et al. used DEM data for drumlin delineation (Eisank, Smith and Hillier 2014); and Eeckhaut et al. used the support vector machine (SVM) algorithm and LiDAR derivatives alone for object-based mapping of landslides in forested terrain (Eeckhaut et al. 2012). SVMs, which are a generalization of linear classifiers, are a set of supervised learning techniques designed to solve discrimination and regression problems.

The use of automated recognition, especially since the advent of convolutional neural networks (CNNs), is becoming more and more widespread in the field of archaeology. Recent work has shown that

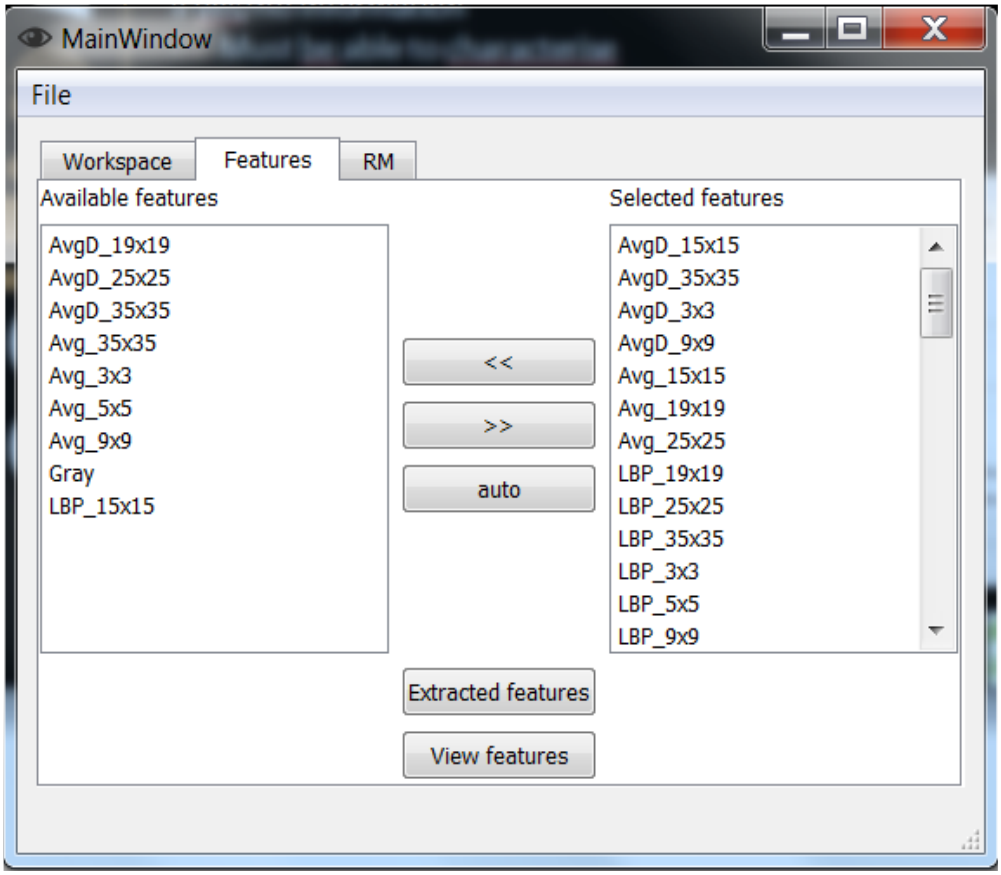

Figure 2. View of the feature selection screen of the human-machine interface (R. Guillaume, C. Laplaige)

this approach can reliably detect slopes, celtic fields, mounds and charcoal burning platforms in LiDAR datasets (Cerrillo-Cuenca 2017; Trier, Cowley and Waldeland 2019; Trier, Salberg and Pilø 2018; Trier, Zortea and Tonning 2015; Vaart and Lambers 2019).

The present work is part of the SOLiDAR project, which is included in the interdisciplinary research and innovation program entitled "Intelligence des Patrimoines". SOLiDAR brings together researchers from several fields (archaeology, history, geology, biology and data processing) and members of the Domaine National de Chambord and the French national forestry commission. It aims to establish data processing protocols aimed at understanding environmental and cultural dynamics to enable the diachronic study of land use. It combines remote sensing data and archaeological, written, geomorphological and ecological sources.

The program is based on a LiDAR survey of a 270-km² area around the city of Blois (Loir et Cher, France) (fig. 1), including the forests of Blois, Boulogne, Russy and the Chambord estate. In this sector, forests cover almost 25,000 ha, comprising 80% of the LiDAR acquisition area, including the Chambord estate, which was created between 1522 and 1650. The earliest mention of these forests dates back to 1176.

The LiDAR acquisition was performed at the beginning of 2015. The average density of ground points is about 10 pts / m², enabling DTM generation with a resolution of 50 cm. For this work, we mainly used a Topographic Position Index (TPI) (annulus, 6m – 20m) on a DTM with a resolution of 2 meters.

For this work, we developed a software application and a human-machine interface (fig. 2), meeting the following criteria:

- the system must be usable by non-specialists, i.e. it must be easy to use, and the human-machine interface (HMI) must be intuitive;
- it must be able to run on any machine and be open source;
- the system must be flexible and adaptable to different types of remains and differ-

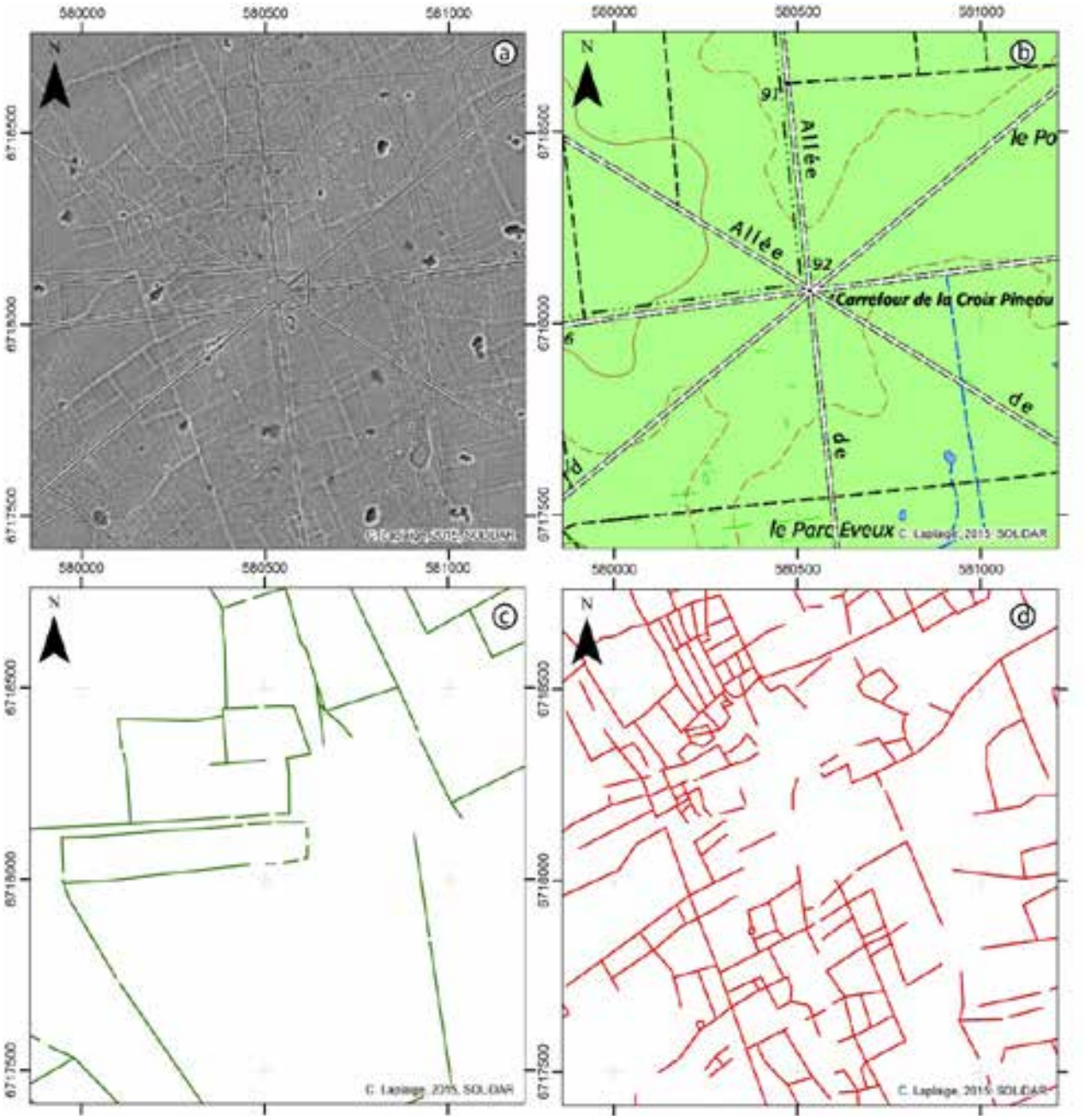

Figure 3. Vineuil, France. a) TPI revealing several micro-reliefs corresponding to archaeological remains; b) current topographic map; c) vectorization of the embankment/ditch system; d) vectorization of the embankment system (C. Laplaige © SOLIDAR, IGN)

ent topographic or geomorphological conditions;

- in order to refine archaeological interpretations, the system must provide a probability of belonging to a type of structure, rather than a presence/absence response;
- finally, the software must be able to characterize the elements that are detected.

The software was developed under Pycharm (https://www.jetbrains.com/pycharm/). It runs under version 3.5.1 of Python and uses the matplotlib 1.5.3, scikit-learn 0.18.1, scikit-image 0.12.3, numpy 1.12.0, scipy 0.19.0 and Sphinx 1.5.1 libraries.

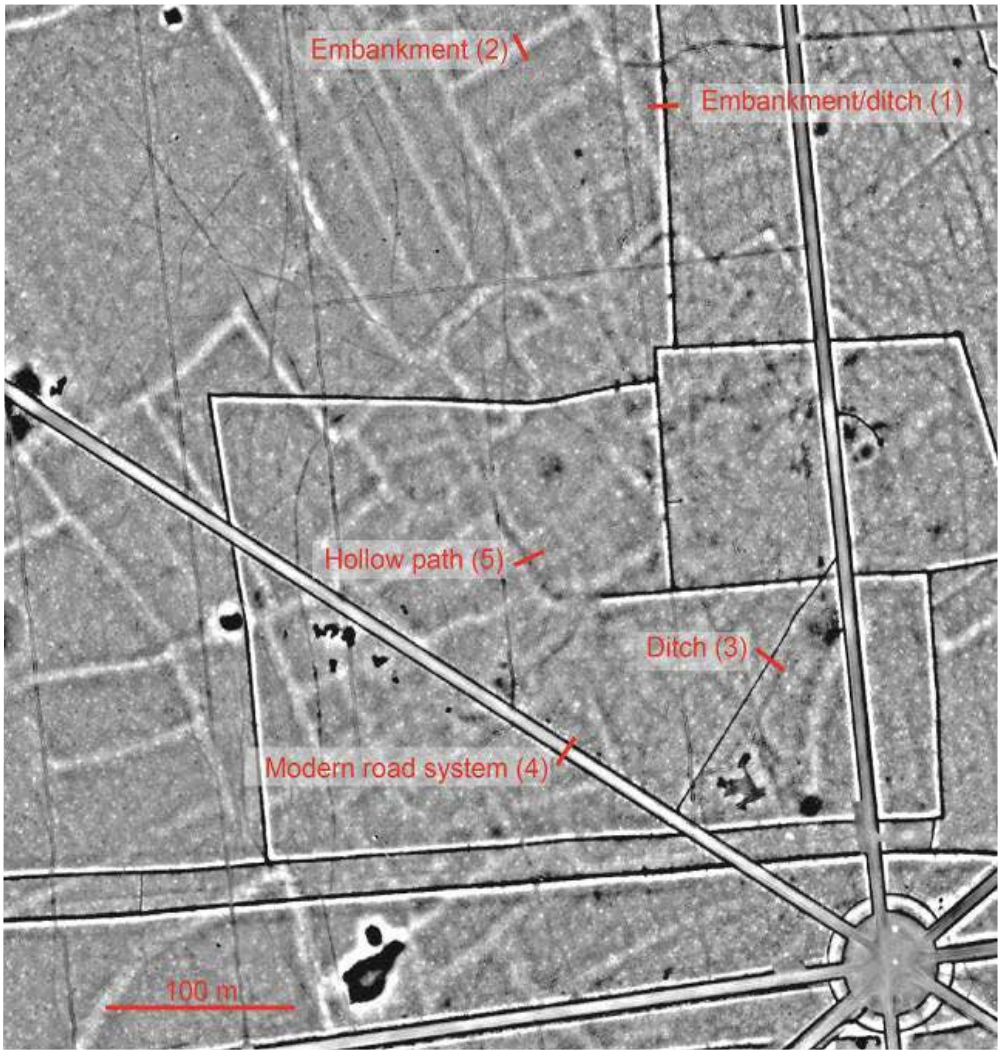

Figure 4. Elements of interest visible on a LiDAR view (C. Laplaige © SOLIDAR)

Types of Remains Investigated

We decided to focus our study on specific Elements of Interest (EOI) for archaeologists, namely linear structures. In the study area, raw LiDAR data analysis revealed at least three overlapping field system patterns (fig. 3).

On the model derived from LiDAR data, we can see in the foreground the current field system (fig. 3b), which overlaps a system of embankments and ditches consisting of rectangular, square or polygonal modules, which may or may not be embedded. In cross-section, the embankment-ditch structure is on average 6 to 8 m wide and less than one meter deep (fig. 3c). These elements were identified by field-walking prior to the LiDAR survey. The embankment-ditch system overlaps a system composed uniquely of embankments, fifteen meters wide and 10-15 cm high (fig. 4 and 5a), unknown before the LiDAR acquisition because the human eye is unable to recognize these features in the field. Some of the most impressive elements can only be seen in situ when specifically looking for them with a background LiDAR map to hand. Unlike the embankment-ditch system, which is composed of large polygonal parcels, this system is composed of tiny rectangles.

The obvious overlap between these three field systems provides an initial indication of relative chronology. The embankment system is the oldest, followed by the embankment/ditch system, and finally the current land occupation structure.

Finally, the morphological changes between these three systems suggest different uses of the space; the current system is based on hunting and forestry activities; the previous embankment/ditch system was possibly used for the same purpose, while the earlier open landscape (embankment system) was probably dedicated to agro-pastoral activities.

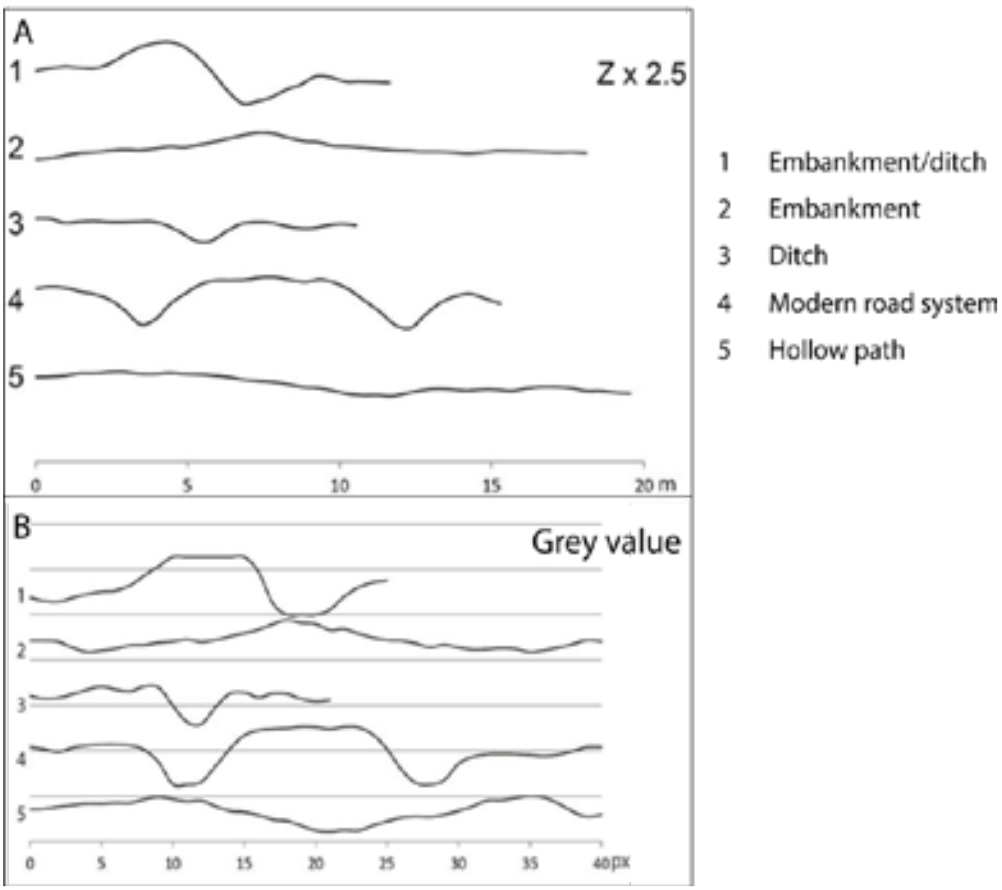

Figure 5. A. Micro-relief anomalies corresponding to features of interest (vertical exaggeration = 2.5). B. Variation of grayscale values on the Topographic Position Index corresponding to elements of interest (C. Laplaige © SOLIDAR)

Analyses of LiDAR data reveal the density of linear elements, most of which were previously undetected; more than 2,000 km have been vectorized manually. Manual digitization of these remains is a time-consuming activity and does not guarantee total recognition of features.

Until recently, LiDAR acquisitions in France were limited to small areas. However, the large-scale reference database recently produced by the French National Geographic Institute now makes vast amounts of very high-resolution data available for areas covering several thousand square kilometers that were previously little known archaeologically, opening the way for the automatic detection of features for archaeological analysis.

Selection of Elements of Interest (EOI)

The objective of the software developed by SOLiDAR is to create a system capable of detecting any type of object; however, for practical reasons and clarity of the present paper, we focus on certain linear structures (see figures 4, 5):

- Embankments/ditches (1), probably corresponding to the previous forestry system. These remains are easily detectable in elevation and in grayscale. In both cases, a steep slope can be observed followed by a depression.

- Embankments (2), corresponding to the earlier system and related to agricultural activities. While not easily discernible in the topography, TPI enables them to be observed in grayscale.

- Ditches (3), with drainage functions. They are easily recognizable by the simple depression.

- Modern road system (4), composed of two ditches, one on either side of a central line of solid ground.

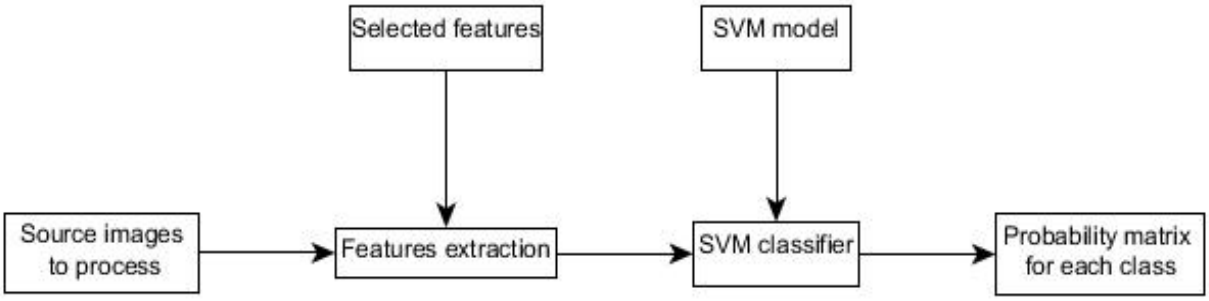

Figure 6. Vineuil, France. a) TPI revealing several micro-reliefs corresponding to archaeological remains; b) current topographic map; c) vectorization of the embankment/ditch system; d) vectorization of the embankment system (C. Laplaige © SOLIDAR, IGN)

Name of element	ditch/ Embankment (1)	Embankment (2)	Ditch (3)	modern	ancient	other	TOTAL
Number	21611	53739	5994	23322	9236	22792	136694

Table I: Summary of the number of pixels integrated in ML processing (S. Bai)

- Probable hollow-way (5). This element is very difficult to recognize in the topography, where it corresponds to a very shallow depression.

Machine Learning Framework

First, we used a conventional image-processing approach to identify the previously defined elements. The goal was to separate the pixels of an initial image into the 5 targeted information layers. Different processing sequences were tested, including: image filtering (median /Gaussian, etc.), multiple thresholding, mathematical morphology operations, connected component analysis, and arithmetic operations between processed DEM and layers. Finally, we examined semi-automated methods based on Machine Learning to create a more flexible and robust framework to characterize archaeological structures from LiDAR derivatives (fig. 6).

Training Step

Selection and Organization of the Training Dataset

The first step involves selecting the input images (DEM) that will be used to compute the pixel features. Based on the expertise of archaeologists and on the results obtained with IP methods, we computed the features using only the Topographic Position Index proposed by Jeff Jenness with a resolution of 2m (Jenness, Brost and Beier 2013). One of our goals is to extract information from other types of visualization (e.g. slope or positive aperture), but this has not yet been achieved.

In the HMI, all that is needed is to define the elements to be detected, and the system creates and organizes the folders. Thereafter, it is necessary to copy the original image and absence/presence images for each element.

For this article, we selected 20 8-bit LiDAR images. For each image, we created 5 binary images (one per class) (fig. 7). The whole set (8-bit image plus the binary images) is used to train the system. We tried to include as many elements as possible and balance the number of pixels for each one (Table I).

Selection of the Features for Pixel Classification

When designing a classification system, the selection of the features to describe the pixels is vital, as well as the content of the training dataset, because they determine the quality of the classification results. We drew up a list of features based on our experience in computer vision. These features are inspired by the well-known and efficient LBP

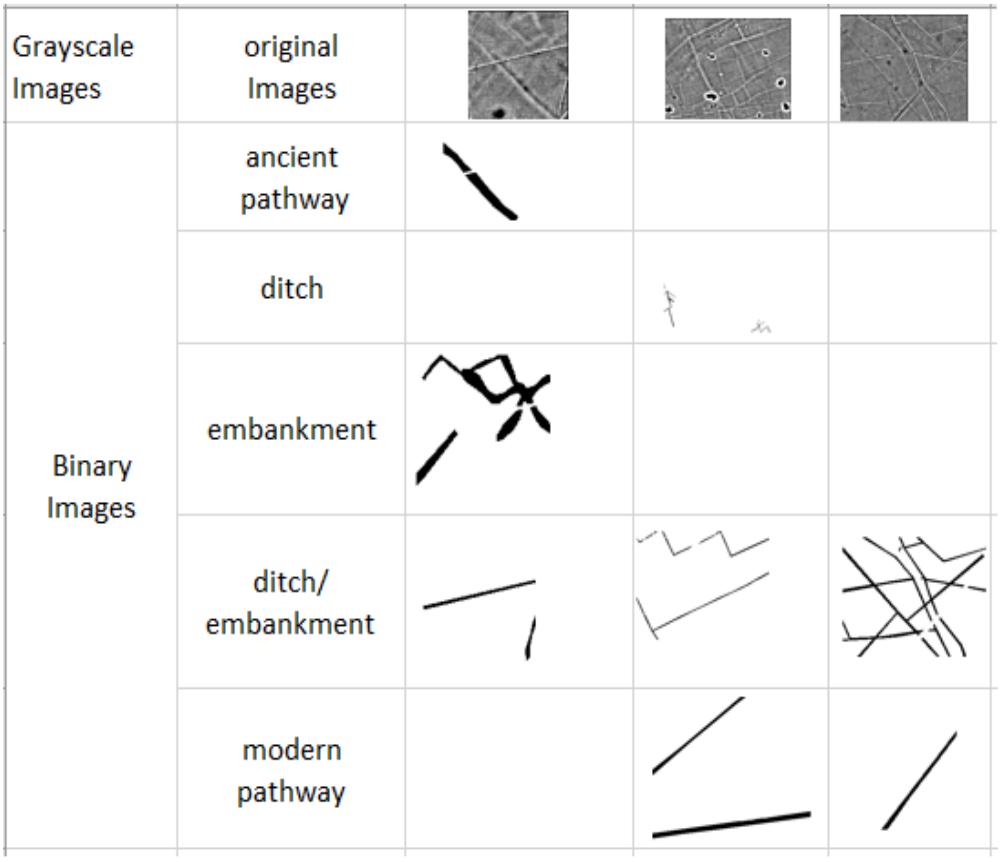

Figure 7. 8-bit TPI extracts and corresponding binary images for each element (S. Bai)

(local binary pattern) method (Ojala, Pietikäinen and Harwood 1996) in which the grayscale values of the local neighborhood are thresholded against the central pixel to provide a binary pattern called texture unit. The number of occurrences of each texture unit is used as descriptors of a region inside an image. We propose an adaptation of this idea to compute the features included in our framework by considering a local neighborhood (of variable mask size) around a central pixel. The features are computed using statistics about grayscale values in different neighborhoods and comparing those values with the value of the central pixel. Currently, the system includes 64 features of 9 types. We think that it should be left to each operator to decide whether to select a feature manually or automatically. In the latter case, features can be selected using a Sequential Forward Floating Selection Method (SFSM) (Pudil, Novovičová and Kittler 1994), which enables different features to be added and subtracted in order to obtain the best possible recognition rate. This rate is calculated by comparing the binary images provided to the system with the detection proposals of the classification algorithm.

Construction of the Classification Model

For the classification, different machine learning algorithms can be adopted and plugged into our framework. For the moment, we have incorporated an SVM classifier in the system. SVM is a non-parametric kernel-based technique based on statistical learning theory, optimization of algorithms, and structural risk minimization theory, and it has been used in many studies. SVM parameters can be optimized using an N-fold cross-validation grid search function.

In this study, since the classes are not linearly separable, a radial basis function (RBF) kernel was used to implement the classification in a higher dimension space. The cost and gamma parameters can be determined by cross-validation.

Once the kernel and major parameters have been set, the SVM model for classification is constructed.

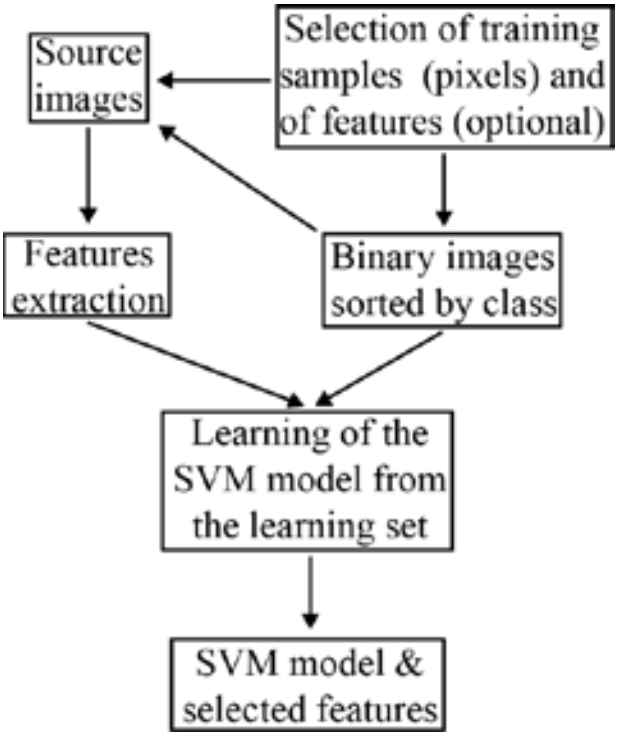

Figure 8. Schematic representation of the SVM Classifier framework (S. Bai, C. Laplaige)

Classification Step

To classify a new image, the first step is to calculate the features of each pixel. The features to use here should be the same as those chosen in step 4.1.2 used to build the SVM model. Those pixels with features are then sent to the SVM model, and the SVM model will calculate the probability of each pixel belonging to each element.

After classification, six probabilities are generated for each pixel, corresponding to 6 classes (5 classes of remains + 1 class of everything else). Probability maps corresponding to all the desired classes of Elements of Interest have to be combined to provide the final decision. Different fusion techniques can be used during this step. In this first study, we used a maximum rule with reject option for the combination and each pixel is assigned to the class with the maximum probability only if the value is higher than a predefined, empirically chosen threshold.

Next, the binary image obtained can be vectorized in a similar way as binary images obtained with a conventional image-processing sequence. This function has not yet been implemented, but we hope to use systems such as those described by Ramel et al. for that purpose (Ramel, Vincent and Emptoz 2000).

First Results

Evaluation Protocols

The position match (PM) was selected to evaluate the EOI inventory map obtained. PM is defined as:

$$PM = \frac{A_{R \cap O}}{A_{R \cup O}} \times 100\%$$

where $A_{R \cup O}$ is the area designated as an EOI either in the reference inventory or in the results, and $A_{R \cap O}$ is the area designated as an EOI in both the reference inventory and in the results, namely, the union (∪) and intersection (∩) of two inventory maps.

A high PM value demonstrates that the two inventories are essentially similar with a good quality of results.

Qualitative Results

An example of processing performed by the SVM is shown in figure 9. On the left, we can see an embankment system, and on the right, the probability of each pixel being an embankment (black corresponds to a 100% probability). We can see that the greatest probability is for the largest remains; the detection of smaller features is less evident. The analysis of this kind of image helps understand the SVM process and improve the system.

Quantitative Results

For this first test, 30,000 samples were used to generate the learning base of SVM, with approximately the same number for each element. The results (PM value %) are displayed in the confusion matrix below (Table II).

The percentage corresponds to remains detected in each class of elements. For example, if we look at the second line, 2% of embankments are detected as other, 50% as embankments, 6% as ditches, etc. For the moment, the error rate is close to 60%. We can see that this is the class with the poorest results, as ancient pathways are particularly difficult to detect,

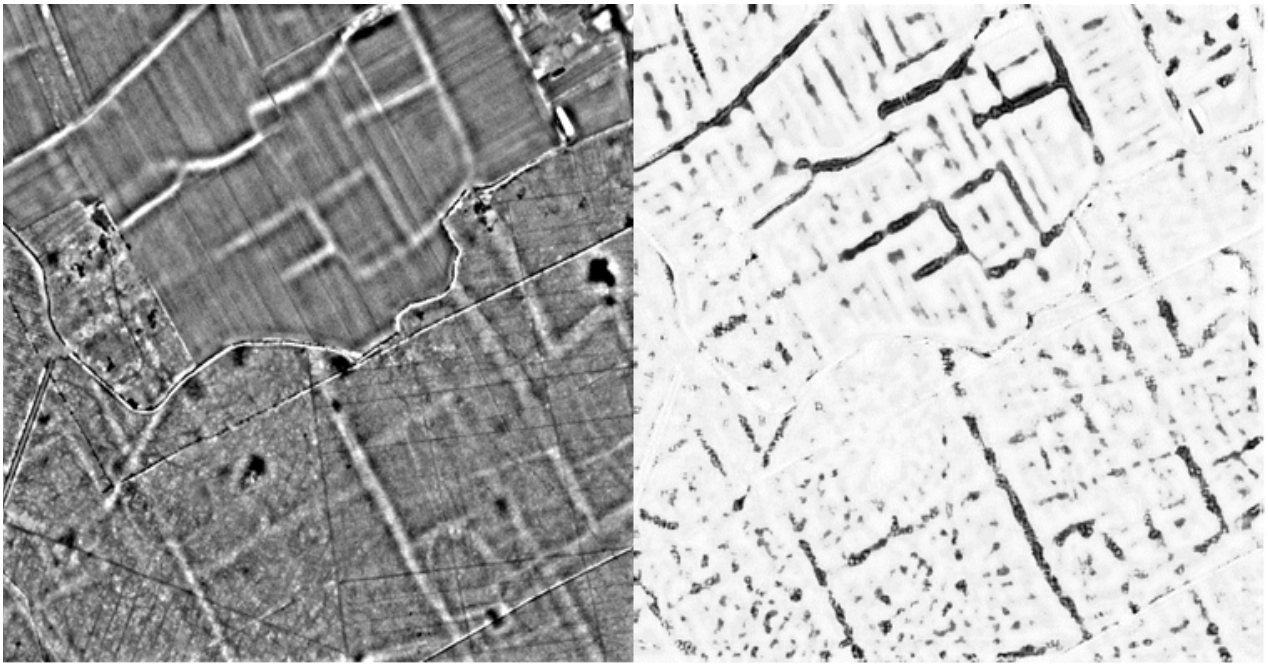

Figure 9. On the left: TPI of an area near Blois. On the right: representation of the probability for each pixel being an embankment (black = 100%, white = 0%) (C. Laplaige)SOLIDAR, IGN)

	Ditch/ embankment (1)	Embankment (2)	Ditch (3)	Modern pathway (4)	Ancient pathway (5)	Other
Ditch/ embankment (1)	40	9	12	22	10	8
Embankment (2)	2	50	6	1	18	23
Ditch (3)	29	1	38	27	4	1
Modern pathway (4)	29	5	5	41	12	6
Ancient pathway (5)	3	35	7	3	28	23
Other	4		6	2	17	31

Table II: Position match value for each element (S. Bai)

	Recall	Precision	F1	MaF1
Ditch/ embankment (1)	0.4	0.37	0.39	0.39
Embankment (2)	0.5	0.36	0.42	
Ditch (3)	0.38	0.45	0.41	
Modern pathway (4)	0.41	0.43	0.42	
Ancient pathway (5)	0.28	0.31	0.29	

Table III: Results of the test

even by an expert. We have not yet found the right features to clearly describe these elements.

We can also see some confusion between modern pathways and embankments/ditches, and between ditches and modern pathways and the embankment/ditch system. It is difficult to differentiate composite

structures using only selected features. In addition to testing new features and looking at vectorization processes to increase the detection rate, it would be interesting to work with fewer types of structures.

We decided to test the ability of this system to classify several types of remains simultaneously (table III). The recall and precision values are between 0.3 and 0.5. The F1 score, which measures the model's performance, has values around 0.4. If we look at the error rate as a whole, it appears that it is higher than the rates reported in other studies (error rate is close to 60%.), for example, for the detection of mounds (Freeland et al. 2016; Sevara et al. 2016). However, the desire to deal with linear rather than isolated objects and to attempt to classify different elements simultaneously effectively limits the overall quality of recognition of the remains.

Conclusion and Outlook

This work is a first attempt to develop a generic Machine Learning framework for the semi-automatic extraction of archaeological elements based on LiDAR DEM. We have created an open-source software application usable by non-specialists. This system, which can be used semi-automatically or manually, can be adapted to different types of remains and to different topographical constraints. The work is in its initial stages, focusing on the extraction of linear structures. It rapidly became clear that the Machine Learning approach has considerable advantages over image processing techniques.

The software has started to be distributed at seminars and will be available for download this summer. The first feedback allowed us to observe a good compatibility of the software on various operating systems and computers. In addition, users with little training in the use of machine learning appreciated the ease of use.

The generation of probabilities rather than binary images from the extraction should allow new databases to be created that can be equally well interpreted. The main idea of this approach is to find a neat way to combine information derived from the DEM (LIDAR data) in order to see whether each pixel is part of a specific Element of Interest. The output of this new framework will be a set of matrices called "probability maps". Each probability map includes the probabilities for each pixel of the image to be part of a specific EOI.

The system is now stable and portable on any type of machine without prior installation, and we can now focus on improving system performance, notably to increase the detection rate. To this end, we are working on several aspects. We wish to add new features and work on several types of LiDAR data visualization. We are looking at the possibility and interest of adding a convolutional neural network to use with our data sets.

Finally, this paper presents only one module of a tool composed of two parts. This module allows you to locate elements of interest freely defined by users in LIDAR data. The output of this module is probability maps of the presence of these elements at the pixel level.

The second module, designed to transform probability maps into vectorized structures (Ramel, Vincent and Emptoz 2000), is currently under development.

References

Anders, N S, Seijmonsbergen, A C and Bouten, W 2013 Geomorphological Change Detection Using Object-Based Feature Extraction From Multi-Temporal LiDAR Data, *IEEE Geoscience and Remote Sensing Letters*, 10(6): 1587–1591. DOI: https://doi.org/10.1109/LGRS.2013.2262317

Baatz, M, Hoffmann, C and Willhauck, G 2008 Progressing from object-based to object-oriented image analysis. In: Blaschke, T, Lang, S, and Hay, G J (eds.) *Object-Based Image Analysis*. Lecture Notes in Geoinformation and Cartography. Springer Berlin Heidelberg. pp. 29–42. DOI: https://doi.org/10.1007/978-3-540-77058-9_2

Blaschke, T 2010 Object based image analysis for remote sensing, *ISPRS Journal of Photogrammetry and Remote Sensing*, 65(1): 2–16. DOI: https://doi.org/10.1016/j.isprsjprs.2009.06.004

Cerrillo-Cuenca, E 2017 An approach to the automatic surveying of prehistoric barrows through LiDAR, *Quaternary International*, 435: 135–145. DOI: https://doi.org/10.1016/j.quaint.2015.12.099

Chen, W, Li, X, Wang, Y, Chen, G and Liu, S 2014 Forested landslide detection using LiDAR data and

the random forest algorithm: A case study of the Three Gorges, China, *Remote Sensing of Environment*, 152: 291–301. DOI: https://doi.org/10.1016/j.rse.2014.07.004

Duro, D C, Franklin, S E and Dubé, M G 2012 A comparison of pixel-based and object-based image analysis with selected machine learning algorithms for the classification of agricultural landscapes using SPOT-5 HRG imagery, *Remote Sensing of Environment*, 118: 259–272. DOI: https://doi.org/10.1016/j.rse.2011.11.020

Eisank, C, Smith, M and Hillier, J 2014 Assessment of multiresolution segmentation for delimiting drumlins in digital elevation models, *Geomorphology*, 214: 452–464. DOI: https://doi.org/10.1016/j.geomorph.2014.02.028

Freeland, T, Heung, B, Burley, D V, Clark, G and Knudby, A 2016 Automated feature extraction for prospection and analysis of monumental earthworks from aerial LiDAR in the Kingdom of Tonga, *Journal of Archaeological Science*, 69: 64–74. DOI: https://doi.org/10.1016/j.jas.2016.04.011

Jenness, J, Brost, B and Beier, P 2013 *Land Facet Corridor Designer: Extension for ArcGIS*. Jenness Enterprises.

Li, X, Cheng, X, Chen, W, Chen, G and Liu, S 2015 Identification of Forested Landslides Using LiDar Data, Object-based Image Analysis, and Machine Learning Algorithms, *Remote Sensing*, 7(8): 9705–9726. DOI: https://doi.org/10.3390/rs70809705

Martha, T R, Kerle, N, Jetten, V, van Westen, C J and Kumar, K V 2010 Characterising spectral, spatial and morphometric properties of landslides for semi-automatic detection using object-oriented methods, *Geomorphology*, 116(1): 24–36. DOI: https://doi.org/10.1016/j.geomorph.2009.10.004

Ojala, T, Pietikäinen, M and Harwood, D 1996 A comparative study of texture measures with classification based on featured distributions, *Pattern Recognition*, 29(1): 51–59. DOI: https://doi.org/10.1016/0031-3203(95)00067-4.

Pudil, P, Novovičová, J and Kittler, J 1994 Floating search methods in feature selection, *Pattern Recognition Letters*, 15(11): 1119–1125. DOI: https://doi.org/10.1016/0167-8655(94)90127-9.

Ramel, J Y, Vincent, N and Emptoz, H 2000 A structural representation for understanding line-drawing images, *International Journal on Document Analysis and Recognition*, 3(2): 58–66. DOI: https://doi.org/10.1007/s100320000037

Sevara, C, Pregesbauer, M, Doneus, M, Verhoeven, G and Trinks, I 2016 Pixel versus object — A comparison of strategies for the semi-automated mapping of archaeological features using airborne laser scanning data, *Journal of Archaeological Science: Reports*, 5: 485–498. DOI: https://doi.org/10.1016/j.jasrep.2015.12.023

Trier, Ø D, Cowley, D C and Waldeland, A U 2019 Using deep neural networks on airborne laser scanning data: Results from a case study of semi-automatic mapping of archaeological topography on Arran, Scotland, *Archaeological Prospection*, 26(2): . DOI: https://doi.org/10.1002/arp.1731

Trier, Ø D, Salberg, A-D and Pilø, L H 2018 Semi-automatic mapping of charcoal kilns from airborne laser scanning data using deep learning. In: *Oceans of Data. Proceedings of the 44th Conference on Computer Applications and Quantitative Methods in Archaeology*. Archaeopress. Oxford: Matsumoto, M and Uleberg, E. pp. 219–231.

Trier, Ø D, Zortea, M and Tonning, C 2015 Automatic detection of mound structures in airborne laser scanning data, *Journal of Archaeological Science: Reports*, 2: 69–79. DOI: https://doi.org/10.1016/j.jasrep.2015.01.005

Vaart, W B van der and Lambers, K 2019 Learning to Look at LiDAR: The Use of R-CNN in the Automated Detection of Archaeological Objects in LiDAR Data from the Netherlands, *Journal of Computer Applications in Archaeology*, 2(1): 31–40. DOI: https://doi.org/10.5334/jcaa.32

Eeckhaut, M van Den, Kerle, N, Poesen, J and Hervás, J 2012 Object-oriented identification of forested landslides with derivatives of single pulse LiDAR data, *Geomorphology*, 173: 30–42. DOI: https://doi.org/10.1016/j.geomorph.2012.05.024

URL

SOLiDAR: http://citeres.univ-tours.fr/spip.php?article2133
Intelligence des patrimoines: https://www.intelligencedespatrimoines.fr
Topographic Position Index: http://www.jennessent.com